

DESIGN OF A PID CONTROLLER FOR A MOLTEN SALT MICROREACTOR

A Thesis

Presented in Partial Fulfillment of the Requirements for the

Degree of Master of Science

with a

Major in Nuclear Engineering

in the

College of Graduate Studies

University of Idaho

by

Sam J. Root

Major Professor: Michael McKellar, Ph.D.

Committee Members: Dakota Roberson, Ph.D.; Robert A. Borrelli, Ph.D.

Department Administrator: Indrajit Charit, Ph.D.

May, 2023

ABSTRACT

Lorem ipsum dolor sit amet, consectetur adipiscing elit. Ut purus elit, vestibulum ut, placerat ac, adipiscing vitae, felis. Curabitur dictum gravida mauris. Nam arcu libero, nonummy eget, consectetur id, vulputate a, magna. Donec vehicula augue eu neque. Pellentesque habitant morbi tristique senectus et netus et malesuada fames ac turpis egestas. Mauris ut leo. Cras viverra metus rhoncus sem. Nulla et lectus vestibulum urna fringilla ultrices. Phasellus eu tellus sit amet tortor gravida placerat. Integer sapien est, iaculis in, pretium quis, viverra ac, nunc. Praesent eget sem vel leo ultrices bibendum. Aenean faucibus. Morbi dolor nulla, malesuada eu, pulvinar at, mollis ac, nulla. Curabitur auctor semper nulla. Donec varius orci eget risus. Duis nibh mi, congue eu, accumsan eleifend, sagittis quis, diam. Duis eget orci sit amet orci dignissim rutrum.

Nam dui ligula, fringilla a, euismod sodales, sollicitudin vel, wisi. Morbi auctor lorem non justo. Nam lacus libero, pretium at, lobortis vitae, ultricies et, tellus. Donec aliquet, tortor sed accumsan bibendum, erat ligula aliquet magna, vitae ornare odio metus a mi. Morbi ac orci et nisl hendrerit mollis. Suspendisse ut massa. Cras nec ante. Pellentesque a nulla. Cum sociis natoque penatibus et magnis dis parturient montes, nascetur ridiculus mus. Aliquam tincidunt urna. Nulla ullamcorper vestibulum turpis. Pellentesque cursus luctus mauris.

ACKNOWLEDGEMENTS

This work and my coursework was completed under a Graduate Fellowship funded by Nuclear Regulatory Commission (NRC). The neutronics modeling was performed through computational resources from the High Performance Computing (HPC) Center at Idaho National Laboratory (INL), with assistance from John Koudelka and the INL HPC support staff.

DEDICATION

To my mother, Tammy, who planted and nurtured my love of science. To my father, Paul, who taught me how to design and build, and showed me that I am an engineer. To my cats, Babe and Bunyan, who stayed up with me all those long nights studying and writing. Thank you for your endless support.

TABLE OF CONTENTS

ABSTRACT	ii
ACKNOWLEDGEMENTS	iii
DEDICATION	iv
TABLE OF CONTENTS	v
LIST OF TABLES	vii
LIST OF FIGURES	viii
LIST OF CODES	ix
LIST OF ACRONYMS	x
CHAPTER 1: INTRODUCTION	1
MICROREACTORS	1
MOLTEN SALT REACTORS	2
MOLTEN SALT NUCLEAR BATTERY	3
SCOPE	3
CHAPTER 2: PROCESS CONTROL ENGINEERING	4
FEEDBACK	4
FEEDFORWARD	5
TRANSPORT DELAY PROBLEM	8
TIME-VARIANCE AND NON-LINEARITY	9
CHAPTER 3: REACTOR CHARACTERIZATION	13
REACTOR DESIGN SELECTION	13
NEUTRONICS MODELING	13
PROCESS SIMULATION	13
CHAPTER 4: CONTROLLER DESIGN	14
CORE POWER TRANSDUCER	14
ACTUATOR	14
REACTOR TRANSFER FUNCTION	14
TUNING METHODOLOGY	14

CHAPTER 5: RESULTS AND ANALYSIS	15
CHAPTER 6: CONCLUSIONS	16
LIMITATIONS	16
FUTURE WORK	16
SUMMARY REMARKS	17
REFERENCES	18
CHAPTER A: TEST	21
CHAPTER B: WHAT	22

LIST OF TABLES

LIST OF FIGURES

1.1	Simplified schematic drawing of an MSNB	3
2.1	Feedback control loop	4
2.2	Feedback control loop with disturbance feedforward	6
2.3	Feedback control loop with pre-filter	7
2.4	Pre-filter on (a) step-function and (b) ramp-function	7
3.1	Control loop of a natural circulation MSNB	13

LIST OF CODES

1	Hello!	21
2	F strings	21

ACRONYMS

HPC High Performance Computing.

INL Idaho National Laboratory.

LTi Linear Time-Invariant.

LWR Light Water Reactor.

MSNB Molten Salt Nuclear Battery.

MSR Molten Salt Reactor.

MSRE Molten Salt Reactor Experiment.

NPP Nuclear Power Plant.

NRC Nuclear Regulatory Commission.

NREL National Renewable Energy Laboratory.

ORNL Oak Ridge National Laboratory.

PID Proportional-Integral-Derivative.

CHAPTER 1

INTRODUCTION

The world is working to move away from fossil fuel as its main energy source [1]. National Renewable Energy Laboratory (NREL) has partnered with over 700 organizations, including large manufacturing companies, to de-carbonize supply chains [2]. Nuclear power has been well established as an alternative for base-load electrical generation with 93 facilities in the United States and 435 globally which each generate on the order of 1 GWe, but there remains a need for smaller reactors to be deployed in more dynamic applications such as small remote grids (including military bases [3]), manufacturing, and power-peaking [4]. These small energy utilizers could turn to microreactors to fill their needs; to make this a reality, a robust control system for microreactors must be designed that is capable of ramping production up and down to meet demand.

1.1 MICROREACTORS

Microreactors, as the name suggests, are small nuclear reactors which are designed to be fully assembled when shipped, rather than constructed on site. This is a hot area of research in the private sector as companies are working to capitalize on the growing need for clean and dependable small scale electrical generation [5]. They aim not to replace the utility scale Nuclear Power Plants (NPPs) which handle base-load electrical generation, but the diesel or natural gas engines that are found at countless manufacturing facilities, peaking stations, military bases, islands, and other locations where on-site generation is the primary or only source of power.

The goal is to deliver a prefabricated microreactor to a site, integrate it to the necessary power cycles and process heat applications, and meet the needs of the site for a long period of time - up to a decade - without the need for refueling or significant maintenance. One of the biggest challenges in implementing microreactors is the transients that these applications often require. Engines handle these quite well, simply adjusting the flow rates of fuel and combustion air. Nuclear reactor load following is a bit more complicated, as the reactor must be made supercritical to ramp up power or subcritical to decrease power. This necessitates characterization of the reactor's criticality control & actuation system and reactivity feedback mechanisms, so an effective 'reactor-following-turbine' controller can be tuned [6, Ch. 8].

1.2 MOLTEN SALT REACTORS

Molten salts are highly desirable in high temperature applications due to their excellent thermophysical properties [7]. Salt mixtures have been developed to have very wide liquid temperature ranges (i.e. low melting point and high vaporization point). They also have very high volumetric heat capacities compared to other high temperature coolants (which tend to be gaseous), and are able to operate at or slightly above ambient pressure. These properties combine to make molten salts excellent choices in heat transfer and thermal storage applications. Furthermore, they are extremely strong electrolytes which can be useful as solvents, catalysts, or reagents in certain chemical reactions including a pyrometallurgical method for reprocessing spent nuclear fuel [8].

Molten Salt Reactors (MSRs) are a family of nuclear reactor in which a fuel salt (containing fissile and/or fertile nuclides) is dissolved in a coolant salt [9]. The concept was proven by the Molten Salt Reactor Experiment (MSRE) at Oak Ridge National Laboratory (ORNL) in the 1960s [10]. It has yet to take off beyond the research reactor sector, but it has re-emerged as a Gen-IV reactor concept, with a team at the Shanghai Institute of Applied Physics gaining approval to operate a now fully constructed thorium breeding MSR [11]. Some of the benefits of MSRs over more conventional LWRs include:

- Higher operating temperatures allow for use in applications requiring high-grade process heat, and yield higher thermal efficiency [9];
- Lower operating pressures contribute to inherent safety, and permit less expensive components [7];
- The ability to burn minor actinides supports the goal of reducing global stockpiles of high-level waste [7];
- Natural circulation of the fuel introduces an additional feedback mechanism that presents the possibility of autonomous load following of certain power demand transients [12];
- There is no concern of core melt-down as the reactor is designed for liquid fuel;
- The liquid state homogenizes nuclides throughout the core, which minimizes burn-up gradient to produce a flatter temperature and power profile within the core [13, Ch. 3]. The flowing nature also allows for online reprocessing, removing fission products and poisons during operation;

They also carry some demerits:

- Molten salts are very corrosive, often requiring more expensive materials [14];
- The chemistry of the coolant (not only the fuel) is constantly changing due to fission, transmutation, and impurities from corrosion;
- Lithium is commonplace in molten salts, so tritium production is unavoidable, being formed by both the ${}^6\text{Li}(n, \alpha){}^3\text{H}$ (Rxn. 1.1) and ${}^7\text{Li}(n, n\alpha){}^3\text{H}$ reaction. Off-gas systems need to be robust to handle tritium as well as radionuclide noble gasses, halides, and inter-halides [15];



1.3 MOLTEN SALT NUCLEAR BATTERY

The Molten Salt Nuclear Battery (MSNB) is a self contained design for a liquid fueled molten salt microreactor [16, 5]. It is fueled by an inorganic form of uranium, UF_4 , dissolved in a coolant salt such as $FLiNaK$ (a eutectic mixture of three alkali fluorides) or $FLiBe$ (a mixture of LiF and BeF_2) [9]. Heat is generated in the core by fission and is rejected in an integrated heat exchanger (Fig. 1.1). Criticality is manipulated using axial control drums, which may be rotated to aim either a neutron reflecting material or a neutron absorbing material towards the core. The design studied in this work is intended to produce up to 1 MWth, although larger designs of up to 50 MWth also exist.

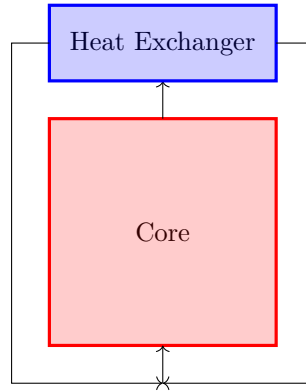


Figure 1.1: Simplified schematic drawing of an MSNB. Heat is generated in the core by fission, is transported by natural circulation of the coolant/fuel salt, and rejected to a secondary working fluid in the heat exchanger before returning to the inlet plenum through the downcomer.

1.4 SCOPE

As a developing design, work has been done on neutronics [5], thermal-hydraulics and autonomous load following [16], and corrosion concerns [17]. However, until now, little to no work has been done on the control system. First and foremost, this work details a multiphysics characterization of the MSNB required to design a feedback controller capable of matching the core power generation to the secondary power demand. In addition to the main control mode of following power transients during normal operation, specific discussion is centered around more dynamic time periods, namely: 1) initial start-up; 2) shutdown, both planned and emergency; and 3) restart;

This work is focused on the operational control system. There are a number of related systems that will also need to be considered, such as: 1) *in-situ* melting of salt immediately following delivery and installation; 2) neutron seed for initial start-up; and 3) decay heat removal for both planned and emergency shut-down; These are important systems but are out of scope for this project.

CHAPTER 2

PROCESS CONTROL ENGINEERING

There are two main goals in process control engineering: 1) Reference tracking, where a process variable is matched to a set-point which may be changed over time; and 2) Disturbance rejection, where the process variable is held to the set-point despite outside influence upsetting it; This is usually achieved by a controller which measures the system inputs and/or outputs using a sensor/transmitter and controls the process variable by manipulating an actuator.

2.1 FEEDBACK

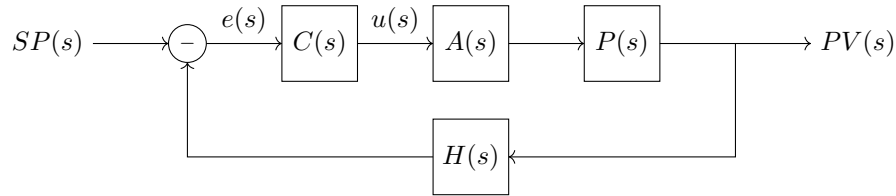


Figure 2.1: Feedback control loop. The process-variable (PV) is measured by the transducer (H) and compared to the set-point (SP). The controller (C) uses the actuator (A) to control the process (P) based on the error (e).

The most common type of controller is a feedback controller. Fig. 2.1 shows a simple feedback control loop with an output sensor/transmitter (*i.e.* transducer), controller, and actuator working together to control a process. The controller takes action (u) based on the ‘error’ (e) between the set-point (SP) and process-variable (PV) (Eqn. 2.1). These systems are typically modeled using transfer functions in the Laplace (or ‘s’) domain.

$$e(t) = PV(t) - SP(t) \quad (\text{Eqn. 2.1})$$

The action, or controller output (u) is often determined by a Proportional-Integral-Derivative (PID) equation (Eqn. 2.2), which considers the instantaneous, cumulative, and predictive error in determining the proper actuation [18, Ch. 5]. This equation has three terms:

- 1) Proportional control term. The control output is manipulated in proportion to the error defined by the proportional gain constant (K_P). A high gain yields an aggressive controller that is prone to overshooting the set-point, while a low gain may result in steady-state offset.
- 2) Integral control term, which considers the historical cumulative error (calculated by taking the time integral of the error) in an effort to eliminate steady-state offset that a P-Only controller may exhibit. As the process variable settles around the set-point, the cumulative error approaches a constant value and the effect of the integral controller diminishes.
- 3) Derivative control term, which estimates the time rate of change of the error to dampen overshoot. This mechanism, sometimes referred to as anticipatory control, slightly reduces the proportional response to the error when the error is changing rapidly. This results in reducing the peak overshoot. A well tuned anticipatory gain can allow a more aggressive proportional gain to be used without the large overshoot.

$$u(t) = \underbrace{K_P e(t)}_{\text{Proportional}} + \underbrace{K_I \int_0^t e(t) dt}_{\text{Integral}} + \underbrace{K_D \frac{de(t)}{dt}}_{\text{Derivative}} \quad (\text{Eqn. 2.2})$$

Instead of using three different gain constants, it is common for controllers to be tuned in terms of a single controller gain (K_C) plus two time constants: 1) The integral time constant (τ_I); and 2) The derivative time constant (τ_D); In this case, Eqn. 2.2 is rewritten as:

$$u(t) = K_C \left(e(t) + \tau_I^{-1} \int_0^t e(t) dt + \tau_D \frac{de(t)}{dt} \right) \quad (\text{Eqn. 2.3})$$

2.2 FEEDFORWARD

The term ‘Feedforward’ can be used to refer to any element in the control block diagram that exists outside of the feedback loop. In process control, feedforward controllers are almost always implemented alongside, not instead of feedback controllers because a standalone feedforward controller is not guaranteed to reach the set-point.

DISTURBANCE FEEDFORWARD

In many processes, the process variable is effected by phenomena other than the actuator. These other phenomena are defined as disturbances. A well-tuned feedback controller is capable of disturbance rejection, but only after the disturbance causes error. In some cases, a disturbance feedforward controller may be added to the feedback controller to cause the actuator to counteract the effect of the disturbance before it occurs [18, Ch. 10]. Fig. 2.2 shows a feedback control loop with the addition of a disturbance feedforward controller.

The most prevalent disturbances that would effect the power output of the core of a MSNB are the temperature reactivity feedback effect common to all nuclear reactors and the flow reactivity specific to natural circulation driven liquid fueled MSRs [12].



Figure 2.2: Feedback control loop with disturbance feedforward. It is identical to Fig. 2.1 with the addition of a disturbance (D) which effects the process variable (PV) according to the disturbance dynamics (P_D), and is measured by the disturbance transducer (H_D). The signal from H_D is sent to the disturbance feedforward controller (C_D) who's output (u_D) is combined with (u) to form the total control output (u^*).

Temperature reactivity feedback is dominated by Doppler Broadening, where the radiative capture resonance peaks of nuclides such as ^{238}U are depressed to cover a wider epithermal neutron spectrum [19, Ch. 2]. This results in a lower resonance escape probability [19, Ch. 3] and a negative correlation between fuel temperature and fuel reactivity. Liquid fuels also have a high thermal-expansion coefficient, so higher core temperatures lead to lower heavy metal density and lower macroscopic fission cross-section in the core [5].

Flow reactivity is driven by the advection of delayed neutron precursors [6, Ch. 3]. Not all fission neutrons are released promptly; sometimes an unstable nuclide which eventually decays by neutron emission produced instead. These unstable nuclides are called delayed neutron precursors and have half-lives ranging from less than a second to over a minute [20, Ch. 7]. An example is given by Rxn. 2.1



Since the fuel in a MSNB is flowing, some delayed neutron precursors will leave the core by advection before the neutron is emitted in a much less reactive part of the reactor. When the temperature differential between the core and primary heat exchanger is increased, the natural circulation flow rate increases too. This decreases the likelihood of delayed neutrons being emitted in the core, and negatively impacts core reactivity. Helix devices meant to elongate the in-core flow path may minimize delayed neutron losses [16].

Disturbance feedforward will not be utilized in the design of the controller outlined in this work. When the outlet temperature of the heat exchanger is decreased, it takes time for the cooler salt to reach the core. The disturbance transport delay is on the order of minutes. Contrastly, Doppler Broadening has a nearly instantaneous effect, so disturbance dynamics are on the order of milliseconds, governed by the mean neutron lifetime [20, Ch. 7]. The effect of control actuation are similarly prompt. Even with a temperature sensor just at the inlet of the core it would be nearly impossible to reliably predict the exact moment that control reactivity would be need to be inserted to counteract the temperature reactivity.

PRE-FILTER

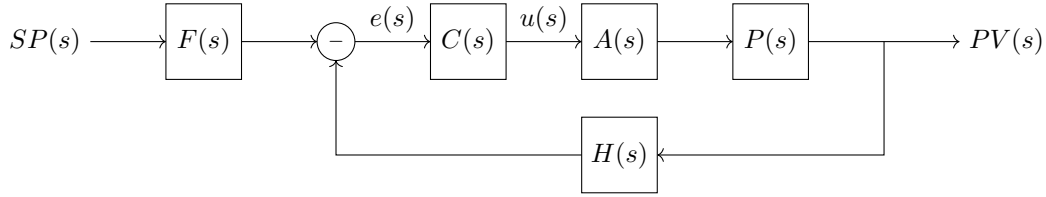


Figure 2.3: Feedback control loop with pre-filter. It is identical to Fig. 2.1 with the addition of the pre-filter (F) which reshapes changes to the set-point (SP) before calculating the error (e).

The control loop for a feedback system with a pre-filter is included as Fig. 2.3. Pre-filters are another type of feedforward mechanism common in control systems. They are typically first-order transfer functions such as Eqn. 2.4 function used to improve the performance of the associated feedback controller (as depicted by Fig. 2.4) by ‘slowing down’ the rate of change of the set-point. The gain (numerator) for a pre-filter is always unity because the desire is only to reshape the input, not resize it. The time-constant (τ_F) describes how quickly the output equilibrates with the input.

$$F(s) = \frac{1}{\tau_F s + 1} \quad (\text{Eqn. 2.4})$$

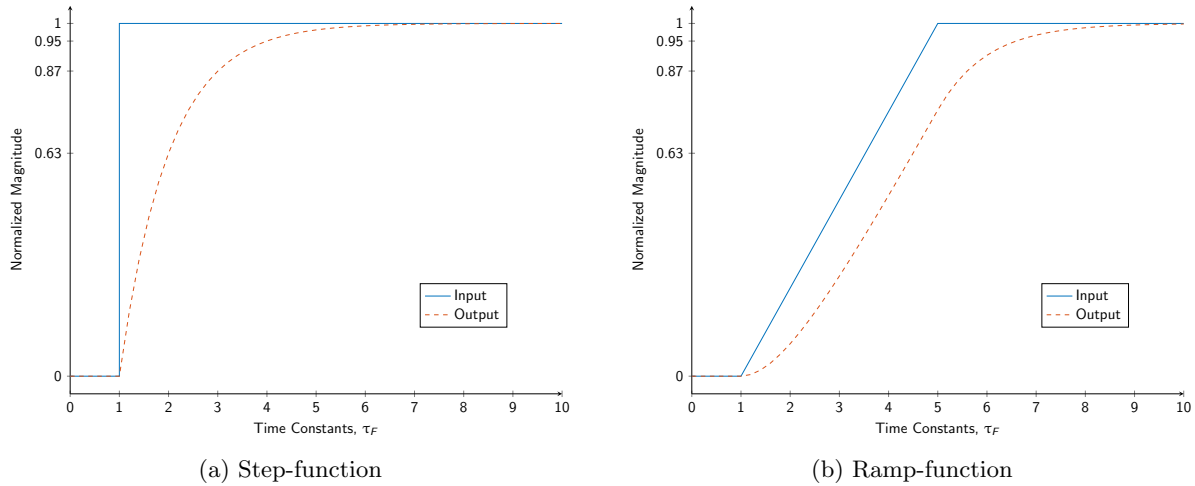


Figure 2.4: Pre-filter on step-function and ramp-function. When the pre-filter acts on a step-function, it follows an exponential curve, reaching 63.2% of the magnitude of the step in 1 time constant, 86.5% in 2 time constants, 95.0% in 3 time constants and so on. The ramp-function exhibits similar but more complicated dynamics due to the changing input.

By resisting instantaneous set-point changes, or step functions, the pre-filter minimizes the instantaneous error during transients and minimizes overshoot by reducing over-actuation or actuator saturation. This is particularly useful in a control system such as the one designed in this report where the set-point is coupled to some other value. In this case, the core power generation needs to match the demand of the secondary system (*e.g.* power cycle). This method allows the secondary system to immediately change

to its necessary value while giving the reactor core time to safely and effectively respond.

The area between the solid blue and dashed orange curves corresponds the net amount of energy expelled from the molten salt loop following the transient. This manifests as a drop in the average salt temperature. If the reactor begins to operate near thermophysical boundaries, it may be necessary for the core to over-produce in order to bring the temperature back up. An alternative approach could be to use a slightly under-damped second-order pre-filter so the core power generation briefly overshoots the heat exchanger power consumption to balance the energy inequality.

2.3 TRANSPORT DELAY PROBLEM

A good place to start in the design of this controller is discussing the dynamics associated with anticipated transients. The prominent factors here are the natural circulation flow mode and the transport delay separating the heat exchanger and core. A common transient for the MSNB is a step-increase in power demand to a steady-state critical MSNB where the core power generation set-point is instantaneously equal to the heat exchanger power consumption. For this thought experiment, consider an ideal controller which produces rapid load following with minimal overshoot.

Need figure(s) here

IMMEDIATE RESPONSE

The heat-exchanger immediately rejects more thermal energy to the secondary loop and the core immediately generates more power. The core outlet temperature increases quite sharply, but since there is a transport delay between the core outlet and heat exchanger inlet (θ_{riser}), this hot salt does not instantaneously reach the heat exchanger, and the heat exchanger outlet temperature drops sharply. Thus, the heat exchanger outlet temperature also drops.

As these hot and cold regions propagate and grow, the natural circulation driving force increases which results in a negative flow reactivity insertion. This is a gradual disturbance which the ideal controller can effectively reject by a counteracting insertion of positive control reactivity.

HEAT EXCHANGER PERTURBATION

Following the response to the initial step-increase, the first notable event occurs when the hot region in the riser reaches the heat exchanger. This produces a hot ‘edge’ in the downcomer temperature profile that lags the cold edge by approximately θ_{riser} , and again disturbs the core through a change in flow reactivity.

CORE PERTURBATIONS

The next event occurs when the cold edge reaches the core inlet, $\theta_{downcomer}$ after the step-increase, causing a rapid insertion of positive temperature reactivity which must be rejected by the controller. θ_{riser} later, the hot edge inserts negative temperature reactivity. Each of these responses cause subsequent temperature edges which rise to the heat exchanger and continue through the system. It is apparent that the ‘ideal’ controller actually inhibits the ability for the reactor to return to steady-state following a transient, instead prolonging both flow reactivity and temperature reactivity oscillations.

A pre-filter that reshapes the core set-point will make the initial hot edge more gradual. Proper tuning of the pre-filter time-constant will allow the reactivity oscillations to decay more quickly. Previous

work [12] has shown that the passive feedback mechanisms (temperature and flow reactivity) are capable of autonomous load following for small transient, though not at the level of performance that may be required in certain applications. Still, this provides the opportunity to minimize fine and rapid actuation while dampening oscillations by using a dead-band; the ‘ringing out’ of minor perturbations could be left to the passive feedback mechanisms after the active feedback controls the bulk of the power change.

2.4 TIME-VARIANCE AND NON-LINEARITY

In control systems, it is typically preferred to work with Linear Time-Invariant (LTI) systems. There are a number of non-linearities and time variances at play in the control of the MSNB which must be handled:

- The Control Drum Angle vs. Reactivity Curve, which describes the relationship between control actuation and system response, is not linear, but sinusoidal [5]. Over small changes to the control drum angle, the curve may be linearized using Taylor Series approximation [18, Ch. 2];
- The core reactivity decreases over the course of months and years due to the depletion of fissile nuclides and the build-up of non-equilibrium neutron poisons [20, Ch. 7]. This means that the bias-point (or unity point) of the control drums will drift away from the absorber shield as the core life evolves. The bias-point, controller gain, and time constants will need to change with time. These parameters may be fit to time functions or, or gain-scheduled using a look-up table, similarly to how autopilot systems for high-altitude aircraft account for the different air properties and mach-number at different altitudes [21];
- The control drums manipulate the criticality of the core, making it supercritical to increase the power, and subcritical to decrease. This is a highly time dependant exponential control mechanism. The derivative control time constant will need to be carefully tuned to minimize the likelihood of significant overshoot following a power transient;

In addition to the relatively slow time variance of fissile fuel depletion during steady-state critical operation, there are specific times in a MSNB’s expected operational life-cycle that exhibit a higher degree of time variance: 1) Start-up; 2) Shut-down; and 3) Re-start.

START-UP

Prior to start-up, it is very likely that the molten salt fuel/coolant mixture will need to be thawed. Initial start-up will also require a neutron source as a seed for the fission chain reaction [19, Ch. 2]. Each of these systems are important considerations for the design of the MSNB and warrant further investigation, but are out of scope for this work and are briefly discussed in Chapter 6.2. The key consideration regarding the start-up control system is the build-up of fission product neutron poisons in the first hours and days of operation.

Xenon Poisoning

^{135}Xe is the strongest known neutron poison, with a microscopic neutron capture cross-section of 2.65 Mb [20, Table II.2]. The concentration of ^{135}Xe is described by a system of differential equations which quantifies the generation, consumption, and decay of itself and its beta-precursor ^{135}I . Equations Eqn. 2.5 and Eqn. 2.6 can be used to track the concentrations of iodine-135 and xenon-135 during start-up, steady-state operation, power transients, shut-down, and dead-time [20, Ch. 7].

$$\frac{dI}{dt} = \underbrace{\gamma_I \Sigma_f^F \phi(t)}_{\text{Fission Yield}} - \underbrace{\lambda_I I(t)}_{\text{Beta Decay}} \quad (\text{Eqn. 2.5})$$

$$\frac{dXe}{dt} = \underbrace{\gamma_{Xe} \Sigma_f^F \phi(t)}_{\text{Fission Yield}} + \underbrace{\lambda_I I(t)}_{\text{Precursor Decay}} - \underbrace{\lambda_{Xe} Xe(t)}_{\text{Beta Decay}} - \underbrace{Xe(t) \sigma_a^{Xe} \phi(t)}_{\text{Radiative Capture}} \quad (\text{Eqn. 2.6})$$

Each nuclide is formed by ^{235}U fission, and removed by beta-decay. Additionally, ^{135}Xe is formed by the beta-decay of ^{135}I and removed by radiative neutron capture¹. Each nuclide builds-up in the reactor until the formation terms, i.e. fission yield and precursor decay, equilibrate with the removal terms, beta decay and radiative capture. By setting the time derivatives to zero, the neutron flux dependent equilibrium concentrations (Eqn. 2.7 and Eqn. 2.8) may be derived algebraically [20, Ch. 7] and can contribute over 2000 pcm of negative poison reactivity to the core.

$$I_\infty(\phi) = \frac{\gamma_I \Sigma_f^F}{\lambda_I} \phi \quad (\text{Eqn. 2.7})$$

$$Xe_\infty(\phi) = \frac{(\gamma_I + \gamma_{Xe}) \Sigma_f^F}{\lambda_I + \sigma_a^{Xe} \phi} \phi \quad (\text{Eqn. 2.8})$$

Samarium Poisoning

The second most important neutron poison to consider after ^{135}Xe is ^{149}Sm . ^{149}Sm is formed by fission² and decays to ^{149}Nd , which is stable, and has a large neutron capture cross-section [20, Ch. 7]. Eqn. 2.9 looks identical to Eqn. 2.5, but Eqn. 2.10 is simpler than Eqn. 2.6 as ^{149}Sm is stable and is not a direct fission product.

$$\frac{dSm}{dt} = \underbrace{\gamma_{Sm} \Sigma_f^F \phi(t)}_{\text{Fission Yield}} - \underbrace{\lambda_{Sm} Sm(t)}_{\text{Beta Decay}} \quad (\text{Eqn. 2.9})$$

$$\frac{dSa}{dt} = \underbrace{\lambda_{Sm} Sm(t)}_{\text{Precursor Decay}} - \underbrace{Sa(t) \sigma_a^{Sa} \phi(t)}_{\text{Radiative Capture}} \quad (\text{Eqn. 2.10})$$

This system too reaches an equilibrium which may be found algebraically where the time derivatives

¹In reality, the decay chain is a bit more complicated than this. ^{135}Te , the direct beta-precursor to ^{135}I is formed by ^{235}U fission [22]. It's half-life is orders of magnitude shorter than ^{135}I , so it is common to neglect its formation and instead lump its fission yield with ^{135}I . ^{135m}Xe is also formed by ^{135}I beta-decay and is neglected for similar reasons.

²As with ^{135}I , ^{149}Sm actually comes from the decay of a much shorter lived nuclide ^{149}Nd . Because neither ^{149}Sm nor ^{149}Nd are strong neutron absorbers, the presence of ^{149}Nd may be neglected in favor of its longer lived daughter product.

are null. Eqn. 2.11 is of the same form as Eqn. 2.7. Interestingly Eqn. 2.12 is independent of the neutron flux in the core. Because it is stable, it is only removed by the same neutron flux that forms it, and contributes a relatively constant 442 pcm of poison reactivity.

$$Pm_{\infty}(\phi) = \frac{\gamma_{Pm}\Sigma_f^F}{\lambda_{Pm}}\phi \quad (\text{Eqn. 2.11})$$

$$Sa_{\infty}(\phi) = \frac{\gamma_{Pm}\Sigma_f^F}{\sigma_a^{Sa}} \quad (\text{Eqn. 2.12})$$

Burnable Poison Control

LWRs are commonly controlled using neutron absorbing additives in two ways [6, Ch. 8]: 1) Burnable poisons (typically poisons whose daughter are neutron-transparent [19, Ch. 14]) are placed in certain fuel rods to flatten the power profile; and 2) Soluble poisons (*i.e.* chemical shim) dissolved in the moderator/-coolant to account for non-equilibrium fission product poison build-up and fissile material depletion.

MSRs may be able to use the intersection of these two concepts; a neutron absorber such as ^{10}B or, ^{155}Gd , or ^{157}Gd may be added to the molten salt mixture to counter-act the poison reactivity built-up by equilibrium poisons like ^{135}Xe and ^{149}Sm . Boron could be added to the salt by dissolving BF_3 gas [23] or sodium fluoroborates such as NaBF_4 [24], either of which could be natural composition or enriched in ^{10}B . Gadolinium could be added as GdF_3 . As the concentration of the fission product poisons build up, the concentration of the burnable poison depletes, and unlike chemical shim, the consumed poison would not be replenished. Making the average core reactivity equivalent upon cold-clean start-up and equilibrium would simplify the gain and bias scheduling early in the fuel lifetime, particularly if a burnable poison can be identified that is burnt at a similar rate as fission product poisons build up.

SHUT-DOWN

Planned shut-down, either for scheduled maintenance or due to a lack of demand, is quite simple. The heat exchanger load is brought to zero or very low power, and the core set-point gradually follows. Careful tuning of the pre-filter time constant can alleviate potential thermal hydraulic (*e.g.* stagnation or reverse-flow) and thermophysical (*e.g.* salt precipitation, freezing, or vaporization) concerns [12]. Whether the reactor is shut down for planned purposes or in an emergency, a decay heat [13] removal system will need to be designed to keep the salt from vaporizing. The emergency shut-down (SCRAM) system and decay heat removal systems are briefly discussed in Chapter 6.2.

RE-START

Compound dynamics in the ^{135}Xe decay chain result in the generation of a large poison reactivity in the hours following a shut-down. This can make restarting the reactor difficult or impossible for a period of approximately two days. When the reactor is shut down, each flux-containing term in the system of ODEs (Eqn. 2.5 and Eqn. 2.6) goes to zero, and the concentrations of the two nuclides are described by the Bateman equations [25], which have a readily available solution (Eqn. 2.13 and Eqn. 2.14), given some initial condition [20]. ^{135}I follows simple exponential decay. ^{135}Xe has a longer half-life than ^{135}I , as well as a lower equilibrium concentration (owing to its huge radiative capture cross-section). This

causes an inverse response, where the ^{135}Xe concentration initially spikes before its population grows and the ^{135}I population shrinks to the point that the rate of ^{135}Xe decay exceeds its formation.

$$I(t) = I_0 e^{-\lambda_I t} \quad (\text{Eqn. 2.13})$$

$$Xe(t) = Xe_0 e^{-\lambda_{Xe} t} + \frac{\lambda_I I_0}{\lambda_I - \lambda_{Xe}} (e^{\lambda_{Xe} t} - e^{\lambda_I t}) \quad (\text{Eqn. 2.14})$$

This system of equations is not ideal, as it results in mandatory reactor dead time. Most nuclear reactors are not designed with enough excess control reactivity to overcome the iodine pit, so they must wait for the xenon to decay. Even if the control system does have the ability to restart during the xenon peak, it can be very unsafe to do so. When the fission chain reaction is restarted, the neutron flux increases and begins transmuting ^{135}Xe . The removal of poisons is akin to positive reactivity insertion [22]. Decreasing poison concentration increases the neutron population and therefore the rate of poison removal. This is a positive feedback system which could run away quickly if control reactivity is not removed to match.

The duration of the xenon spike may be shortened by adding an additional negative term to Eqn. 2.6. This is not physically realizable in cladded solid fuel reactors. It is however possible to remove a gaseous solvent from a liquid (such as MSR fuel) through a process called stripping [26, Ch. 10]. Helium may be bubbled through the molten salt in a sparge tube, and the xenon (as well as any other fission gasses [27]) would preferentially transport into the gaseous phase which would later be separated in a cyclone or similar apparatus [28]. This advective removal of ^{135}Xe would allow the MSNB to be restarted without having to wait for the poison to decay. ^{149}Sa is stable and strongly dissolved in the molten salt, so it is always ‘burnt off’ during restart [20, Ch. 7].

REACTOR CHARACTERIZATION

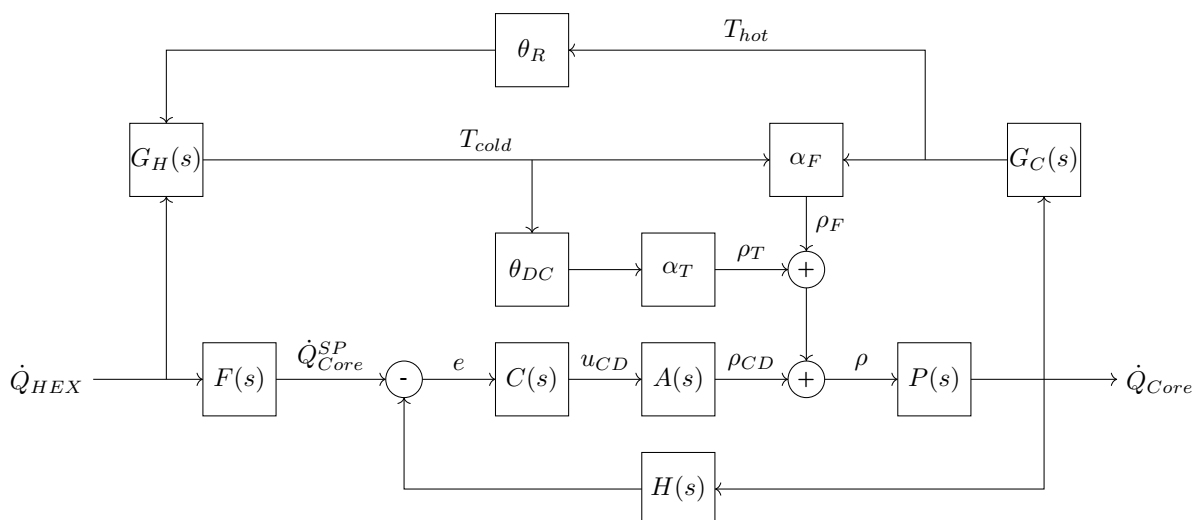


Figure 3.1: Control loop of a natural circulation MSNB. It is a normal feedback loop with a pre-filter, with the addition of the passive feedback mechanisms. The core (\dot{Q}_{Core}) and heat exchanger (\dot{Q}_{HEX}) powers go through the respective temperature dynamics (G_C and G_H) and time delays for the riser (θ_R) and downcomer (θ_{DC}) before being converted to reactivity by the temperature (α_T) and flow (α_F) feedback mechanisms. The passive reactivity feedback is combined with the control drum reactivity (ρ_{CD}) and fed into the reactor dynamics ($P(s)$).

3.1 REACTOR DESIGN SELECTION

3.2 NEUTRONICS MODELING

3.3 PROCESS SIMULATION

CHAPTER 4

CONTROLLER DESIGN

4.1 CORE POWER TRANSDUCER

4.2 ACTUATOR

4.3 REACTOR TRANSFER FUNCTION

4.4 TUNING METHODOLOGY

CHAPTER 5

RESULTS AND ANALYSIS

CHAPTER 6

CONCLUSIONS

6.1 LIMITATIONS

6.2 FUTURE WORK

FUEL SALT THAWING

Because microreactors are meant to be delivered in a fully or mostly assembled state, it is likely that the MSNB will be shipped with the molten fuel/coolant salt mixture frozen *in-situ*. The salt will need to be melted before initial start-up, and the heat source for melting the cannot be fission, as the MSNB requires advective heat removal caused by natural circulation; this is not possible if the flow channels between the core and heat exchanger are frozen. One possible method for salt thawing involves passing low-voltage high-current electricity through the pipes in contact with the salt, similar to how frozen water pipes are thawed [29]; this would be coupled with the introduction of hot secondary coolant into the heat exchanger to provide the necessary hot reservoir.

NEUTRON SOURCE

A neutron source will be required to start the fission chain reaction after installation, and after any long periods of inactivity. ^{235}U undergoes spontaneous fission [30, Ch. 6], and at high enrichment may be used as the only neutron seed simply by putting the control actuators in a supercritical orientation. More commonly, a dedicated source is used, such as ^{252}Ca , which undergoes spontaneous fission much more rapidly, or a composite of a strong alpha-emitter (*e.g.* ^{238}Pu , ^{241}Am , ^{210}Po , or ^{226}Ra) and ^9Be which emits a neutron according to Rxn. 6.1 [31, Ch. 2]. Dedicated neutron seed materials composed of these nuclides could be placed in the core through specialized mechanisms, though the introduction of the seed species as a soluble salt warrants a feasibility analysis.



SCRAM SYSTEM

The emergency shutdown (*i.e.* SCRAM) system must be passive. In LWRs, this is achieved by including large control rods which are actively held out of the core, so that a loss of power results in automatic insertion. Larger MSR designs may include a SCRAM tank into which the fuel/coolant salt drains in the event of power failure. These systems are often actuated by a freeze plug [32] and put the salt in a subcritical orientation by the inclusion of neutron control materials [33, Ch. 1] and high geometric buckling [20, Ch. 6].

In the MSNB, the control drums will be actively actuated such that loss of power results in a negative control reactivity insertion of the greatest possible magnitude. Still, a freeze plug SCRAM tank system should also be included to make the system truly fail-safe

how to emphasize
that this is author
opinion

DECAY HEAT REMOVAL

Thermal power continues to be released by the decay of radio-nuclides after the fission chain reaction is stopped. For non-emergency shut-down, this heat may be removed by the same heat exchanger used for the secondary loop. There should also be a passive system that rejects decay heat in the event of total power failure, such as a direct contact system which removes heat through the vaporization of sodium [34] in the scram tank. This latent heat driven system is ideal because it minimizes the possibility of the salt freezing due to over-cooling.

FLOW RATE CONTROL

6.3 SUMMARY REMARKS

REFERENCES

- [1] Valluri, Sriram Kumar, 2021. Carbon Capture and Utilization. Ph.D. thesis, Michigan Technological University.
- [2] NREL, 2021. Technology partnerships. Technical report, National Renewable Energy Laboratory (NREL).
- [3] Secretary of the Air Force, Public Affairs, 2022. Request for proposal released for eielson air force base micro-reactor pilot program. Energy Installations and Environment.
- [4] Nuclear Energy Institute, 2018. Roadmap for the deployment of micro-reactors for u.s. department of defense domestic installations. Technical report, Nuclear Energy Institute.
- [5] Peterson, John, 2019 8. An Analysis of the Nuclear Characteristics of a Molten Salt Microreactor. Master's thesis, University of Idaho.
- [6] Kerlin, Thomas W., Upadhyaya, Belle R., 2019. Dynamics and Control of Nuclear Reactors. Elsevier Inc., Knoxville, Tennessee.
- [7] Roper, Robin, Harkema, Megan, Sabharwall, Piyush, Riddle, Catherine, Chisholm, Brandon, Day, Brandon, Marotta, Paul, 2022. Molten salt for advanced energy applications: A review. Annals of Nuclear Energy 169, 108924. ISSN 0306-4549. doi:<https://doi.org/10.1016/j.anucene.2021.108924>. URL <https://www.sciencedirect.com/science/article/pii/S030645492100801X>
- [8] Simpson, Michael F., 2012. Development of spent nuclear fuel pyroprocessing technology at Idaho National Laboratory (INL). Technical report, Idaho National Laboratory (INL).
- [9] Roper, Robin V., Sabharwall, Piyush, Christensen, Richard, 2019. Chemical overview of molten salts. ANS Annual Meeting. URL <https://www.ans.org/pubs/transactions/article-45524/>
- [10] Haubenreich, P N, Engel, J R, Prince, B E, Claiborne, H C, 1964 2. Msre design and operations report. part iii. nuclear analysis. Technical report, Oak Ridge National Laboratory. doi:10.2172/4114686. URL <https://www.osti.gov/biblio/4114686>

- [11] World Nuclear News, 2022. Chinese molten-salt reactor cleared for start up. World Nuclear News. URL <https://www.world-nuclear-news.org/articles/chinese-molten-salt-reactor-cleared-for-start-up>
- [12] Carter, John P., Christensen, Richard, Yoon, Sujong, 2022. Numerical analysis of dynamic load following response in a natural circulation molten salt power reactor system. Nuclear Engineering and Design .
- [13] Todreas, Neil E., Kazimi, Mujid S., 1990. Nuclear Systems Volume I: Thermal Hydraulic Fundamentals. Taylor and Francis, USA.
- [14] Roper, Robin V., Christensen, Richard, 2019. Redox potential control for the molten salt reactor concept. ANS Winter Meeting. URL <https://www.ans.org/pubs/transactions/article-47571/>
- [15] Andrews, Hunter B., McFarlane, Joanna, Chapel, A. Shay, Ezell, N. Dianne Bull, Holcomb, David E., de Wet, Dane, Greenwood, Michael S., Myhre, Kristian G., Bryan, Samuel A., Lines, Amanda, Riley, Brian J., Felmy, Heather M., Humrickhouse, Paul W., 2021. Review of molten salt reactor off-gas management considerations. Nuclear Engineering and Design 385, 111529. ISSN 0029-5493. doi: <https://doi.org/10.1016/j.nucengdes.2021.111529>. URL <https://www.sciencedirect.com/science/article/pii/S0029549321004817>
- [16] Carter, John P., 2022. Multi-Physics Investigation of a Natural Circulation Molten Salt Micro-Reactor that Utilizes an Experimental In-pile Device to Improve Core Physics and System Thermal-Hydraulic Performance. Ph.D. thesis, Univesity of Idaho.
- [17] Roper, Robin, 2022. The Effect of Impurities and Geometry on the Corrosion and Thermodynamic Behavior of Molten Salts. Ph.D. thesis, Univesity of Idaho.
- [18] Bequette, B. Wayne, 2003. Process Control: Modeling Design and Simulation. Pretice Hall, Upper Sadle River, New Jersey.
- [19] Duderstadt, James J., Hamilton, Louis J., 1976. Nuclear Reactor Analysis. Wiley & Sons, New York, NY, 1st edition.
- [20] Lamarsh, John R., Baratta, Anthony J., 2001. Introduction to Nuclear Engineering. Pretice Hall, Upper Sadle River, New Jersey, 3rd edition.
- [21] Gahinet, Pascal M., Apkarian, Pierre, 2013. Automated tuning of gain-scheduled control systems. IEEE Conference on Decision and Control. URL <https://ieeexplore.ieee.org/document/6760297>
- [22] Al Rashdan, Ahmad, Roberson, Dakota, 2019. A frequency domain control perspective on xenon resistance for load following of thermal nuclear reactors. IEEE Transactions on Nuclear Science 66(9), 2034. doi:10.1109/TNS.2019.2934171.

- [23] Shaffer, J. H., Grimes, W. R., Watson, G. M., 1962. Boron trifluoride as a soluble poison in molten salt reactor fuels. *Nuclear Science and Engineering* 12(3), 337.
- [24] Koger, J.W., Litman, A.P., 1970. Compatability of fused sodium fluoroborates and BF_3 gas with hastelloy n alloys. U.S. Atomic Energy Commission .
- [25] Ding, Zechaun, 2019. Solving bateman equation for xenon transient analysis using numerical methods. *Nuclear Engineering and Technology* .
- [26] Geankoplis, Christie J., 1993. Transport Processes and Unit Operations. Prentice Hall, Englewood Cliffs, New Jersey, 3rd edition.
- [27] Andrews, Hunter B., McFarlane, Joanna, Chapel, A. Shay, Ezell, N. Dianne Bull, Holcomb, David Eugene, de Wet, Dane, Greenwood, Michael S., Myhre, Kristian G., Bryan, Samuel A., Lines, Amanda, Riley, Brian J., Felmy, Heather M., Humrickhouse, Paul W., 2021 10. Review of molten salt reactor off-gas management considerations. *Nuclear Engineering and Design* 385. doi:10.1016/j.nucengdes.2021.111529.
- [28] Peebles, F.N., 1968. Removal of xenon-135 from circulating fuel salt of the msbr by mass transfer to helium bubbles. U.S. Atomic Energy Commission .
- [29] Bohlander, Thomas W., 1963. Electrical method for thawing frozen pipes. *Journal AWWA* 55(5), 602. doi:<https://doi.org/10.1002/j.1551-8833.1963.tb01056.x>.
URL <https://awwa.onlinelibrary.wiley.com/doi/abs/10.1002/j.1551-8833.1963.tb01056.x>
- [30] Shultis, J. Kenneth, Faw, Richard E., 2002. Fundamentals of Nuclear science and Engineering. Marcel Dekker Inc., New York City, New York, 1st edition.
- [31] Kok, Kenneth D., 2009. Nuclear Engineering Handbook. Taylor & Francis Group, Boca Raton, Florida, 1st edition.
- [32] Tiberga, Marco, Shafer, Devaja, Lathouwers, Danny, Rohde, Martin, Kloosterman, Jan Leen, 2019. Preliminary investigation on the melting behavior of a freeze-valve for the molten salt fast reactor. *Annals of Nuclear Energy* 132, 544. ISSN 0306-4549. doi:<https://doi.org/10.1016/j.anucene.2019.06.039>.
URL <https://www.sciencedirect.com/science/article/pii/S0306454919303573>
- [33] Murty, K. Linga, Charit, Indrajit, 2013. An Introduction to Nuclear Materials: Fundamentals and Applications. Wiley-VCH, Ralieggh, NC.
- [34] Wang, Shisheng, Massone, Mattia, Rineiski, Andrei, Merle-Lucotte, E., Laureau, A., GÃ©rardin, D., Heuer, D., Allibert, M., 2019. A passive decay heat removal system for emergency draining tanks of molten salt reactors. *Nuclear Engineering and Design* 341, 423. ISSN 0029-5493. doi: <https://doi.org/10.1016/j.nucengdes.2018.11.021>.
URL <https://www.sciencedirect.com/science/article/pii/S0029549318309567>

APPENDIX A

TEST

Code 1: Hello!

```
1 print("Hello World") #comment
2 try:
3     a=2/x
4 except ZeroDivisionError:
5     print('undefined')
```

Inline codes like `import` numpy

Code 2: F strings

```
1 x = 4
2 print(f"The numeral four: {x}")
3 #comment
```

APPENDIX B

WHAT

Straight Cash Homie